SUPPORTING INFORMATION

Analysis of Inorganic Polyphosphates by Capillary Gel Electrophoresis

Andrew Lee and George M. Whitesides*

Department of Chemistry and Chemical Biology, Harvard University

12 Oxford St., Cambridge, MA, U.S.A.

*****Author to who correspondence should be addressed:

E-mail: gwhitesides@gmwgroup.harvard.edu

EXPERIMENTAL SECTION.

Sources of Chemicals and Reagents. All chemicals were reagent grade unless stated otherwise. Samples of polyphosphate glass and sodium polyphosphate were purchased from Sigma-Aldrich (St. Louis, MO). Samples of polyphosphoric acid were provided by Rhodia (Birmingham, U.K.). Tris, bis-tris, terephthalic acid, 3-methacryloxy-propyltrimethoxysilane, ammonium bicarbonate, potassium chloride, poly(ethylene glycol) (PEG, average molecular weight 1500 g/mol) and urea were purchased from Sigma-Aldrich. Poly(*N*,*N*-dimethylacryalmide) (PDMA) was purchased form Polymer Source Inc. (Montreal, Canada). Dowex-2 anion exchange resin, Dowex MR-3 Marathon mixed-bed ion exchange resin, and Chelex 100 (sodium form) were purchased from Sigma-Aldrich. The copolymer of *N*,*N*-dimethylacrylamide and 3-methacryloxy-propyltrimethoxysilane was prepared using a method reported by Cretich et.al. (Ref. 79 in the text). Briefly, dimethylacrylamide (mol fraction 0.99) and 3-methacryloxy-propyltrimethoxysilane (mol fraction 0.01) were mixed in a solution of tetrahydrofuran (THF) and polymerized by azo-(bis(isobutyronitrile) (AIBN) at 60 °C. Material was precipitated twice from hexanes twice, dried under vacuum, and used without further purification.

Running Buffer and Solutions of Gel. For CZE, stock solutions of running buffer were prepared by dissolving terephthalic acid (to a final concentration of 9.0 mM) in solutions of tris (56.0 or 72.0 mM) or bis-tris (56.0 or 72.0 mM). Stock solutions were diluted three-fold, degassed by freeze-pump-thaw, and filtered (0.2 μm cutoff) prior to use. For CGE experiments, solutions of gel were prepared by mixing running buffer with a stock solution of PDMA (22.5% w/vol) that had been treated with Chelex for removal

of trace metal impurities. Prior to pumping into capillaries, solutions of gel were degassed by freeze-pump-thaw, and centrifuged for five minutes at 14,000 G. Solutions for buffer reservoirs were prepared from stock solutions of running buffer and a stock solution of PEG that had been treated with mixed-bed ion exchange resin, for removal of traces of ion impurities; solutions were degassed by freeze-pump-thaw immediately before use.

Capillary Coating. For both CZE and CGE experiments, we used fused-silica capillaries (57 cm in length, 50 cm between inlet and detector, 100 μm internal diameter; Polymicro Technologies – Phoenix, AZ) that had been coated with a copolymer of *N*,*N*-dimethylacrylamide and 3-methacryloxy-propyltrimethoxysilane ("copolymer"), for suppression of electroosmotic flow. We used the following procedure to prepare coated capillaries: i) rinse with 1.0 M NaOH for 10 min.; ii) rinse with H_2O for 10 min.; iii) pump in solution of 0.6% (w/vol) of copolymer and 12% $(NH_4)_2SO_4$ for 10 min.; iv) place capillary into oven set to 70 °C for 5 hours; v) rinse with H_2O; capillaries were store at 4 °C when not in use. Capillaries prepared this way had electro-osmotic flow < 0.1 $cm^2\ kV^{-1}\ min^{-1}$ and were used in > 200 experiments, over the course of several months, without observable change.

Capillary Electrophoresis. CZE experiments: Prior to analysis of samples, capillaries were filled with solutions of running buffer and equilibrated at 14.6 kV for 60 min. (cathode at the inlet). In a typical experiment, sample ions were added by electrokinetic injection (2.0 s at 10 kV), followed by dipping the inlet into a vial filled with running buffer (to rinse the outside of the inlet), and separated by electrophoresis at 14.6 kV. CGE experiments: Prior to analysis of samples, capillaries were filled by

pumping in solutions of PDMA for 20 min. at 30 psi, and equilibrated at 14.6 kV for 20 min.. Procedures for sample injection and analysis were the same as those for CZE.

ADDITIONAL BACKGROUND.

Biochemistry of $(P_i)_n$.

Polyphosphate Kinases (PPK). The recently solved crystal structure of PPK1 from *E. coli* identified an ATP-binding site, a histidine residue that is phosphorylated in the first step of the overall reaction, and a channel within the enzyme that allows for the association of $(P_i)_n$ and translocation during reaction.[1] Analyzing $(P_i)_n$ by PAGE provided a way to characterize the synthesis of $(P_i)_n$ from ATP (the reverse reaction in Eq. 1 in the text) catalyzed by PPK (from *E. coli*, *P. aeruginosa*, or *P. shermanii*).[2] The distribution in chain length of synthesized $(P_i)_n$ ($n > 200$) indicated a processive reaction, and the biosynthesis of $(P_i)_n$ by chain growth.

Phosphoglucokinase catalyzes the transfer of phosphate residues from either ATP or $(P_i)_n$ to glucose. Analysis of $(P_i)_n$ in enzyme-catalyzed reactions showed both processive and non-processive utilization of $(P_i)_n$, and a dependence on the chain length of $(P_i)_n$.[3] The consumption of $(P_i)_n$ with $n \sim 450$ was processive. In the analysis of reactions consuming $(P_i)_n$ with $n < 100$, the appearance of ladders of $(P_i)_n$ with lower values of n suggested the dissociation of $(P_i)_n$ from the enzyme and a non-processive mechanism. The consumption of $(P_i)_n$ with $n < 100$ was also less rapid than $(P_i)_n$ with $n \sim 450$.

The resolution of $(P_i)_n$ by ion-exchange chromatography enabled the comparison of reactions of two different mixtures of $(P_i)_n$ – one containing $\sim P_1$-P_{30} and a second containing $\sim P_{10}$-P_{40} – catalyzed by PPK1 from *E. coli*.[4] The extent of reaction for $\sim P_{10}$-

P_{40} was higher (80% reacted) than for ~ P_1-P_{30} (40%). Both reaction mixtures accumulated P_2 and P_{10}. The results indicate a specificity of PPK with chain length, with PPK unable to act upon short chain $(P_i)_n$ ($n < 10$). Observation of decreasing amounts of $(P_i)_n$ and changes in the distribution in chain length (median values of *n* decreased from 60 to 20, determined by PAGE) in mutants of *S. cerevisiae* allowed Ogawa et. al. to identify the function of genes PHM1 – PHM4 in the accumulation and synthesis of $(P_i)_n$ in response to starvation in P_i.[5]

Regulatory role. Studies of mutants of *E. coli* and *P. aeruginosa* with decreased levels of PPK activity showed impairment in several functions, including survival in stationary phase, response to starvation, motility, and the biosynthesis of alginate. This range of phenotypes suggested a potential regulatory role for $(P_i)_n$, via induction of the expression of the sigma factor *rpoS* or participation in signal transduction pathways.[1,6-7] The molecular basis, including the specific interactions of $(P_i)_n$ with proteins, was not known in these examples.

Other roles of $(P_i)_n$ in Biology. The discovery of $(P_i)_n$ in biological systems began with the observation of dense granules by histochemical staining.[1] These particles consisted of $(P_i)_n$ complexed with Ca^{2+} and Mg^{2+}; their composition suggested a function of storing intracellular $(P_i)_n$ or Ca^{2+} and Mg^{2+} in insoluble form. Discovery of a eukaryotic PPK (*D. discoideum*) led to a possible connection between $(P_i)_n$ and the structural biology of *D. discoideum*.[8] PPK from *D. discoideum* probably consists of three actin-related proteins. The synthesis of $(P_i)_n$ catalyzed by PPK from ATP was concurrent with the transition of the protein from globular to filamentous form, resulting in the assembly of filaments (> 500 nm in length) associated with PPK activity.

Materials Properties.

Condensed inorganic phosphate is a commercial material.[9] The production of $(P_i)_n$ has been driven by its inclusion in fertilizer, food products, detergent formulations, and building materials. These applications take advantage of several characteristic chemical and material properties of $(P_i)_n$, including its ability to serve as a phosphate source, metal chelator, or flame retardant.

Samples Zones, Shapes of Peaks, and Areas of Peaks Observed by Indirect UV Absorbance.

Detection of $[(P_i)_n]$ by Changes in $[TP^{2-}]$. Within a sample zone, the current generated by the migration of analyte ions supplements the current generated by the migration of TP^{2-}. The difference in concentration of TP^{2-} within a sample zone ($[TP^{2-}]$) and in the running buffer ($[TP^{2-}]_0$), $\Delta[TP^{2-}]$, depends on the concentration of analyte *i* in the sample zone ($[i]_{CE}$), the amount of negative charge on *i* and TP^{2-} (z_i and z_{TP2^-}), the mobility of *i* and TP^{2-} (μ_i and μ_{TP2-}), and the mobility of the cation in the running buffer (μ_{C+}) (Eq. 1). Derivation of Eq. 1, beginning with the conditions of electroneutrality and the Kohlrausch regulating function, is available in reviews of indirect detection in capillary electrophoresis.[10]

$$\Delta[TP^{2-}] = [i]_{CE} \cdot \left(\frac{z_i}{z_{TP^{2-}}} \right) \cdot \left(\frac{\mu_{TP^{2-}}}{\mu_i} \right) \cdot \left(\frac{\mu_{C^+} + \mu_i}{\mu_{C^+} + \mu_{TP^{2-}}} \right) \qquad (1)$$

The quantity $\Delta[TP^{2-}][i]_{CE}^{-1}$ is known as the transfer ratio, and characterizes the sensitivity of $[TP^{2-}]$ to *i*. Scheme 1 illustrates examples for the detection of ions by $\Delta[TP^{2-}]$ at sensitivities determined by the mobility and charge of the analyte.

Scheme 1. Indirect Detection of Anions with Changes in Concentration of TP^{2-} in Samples Zones.

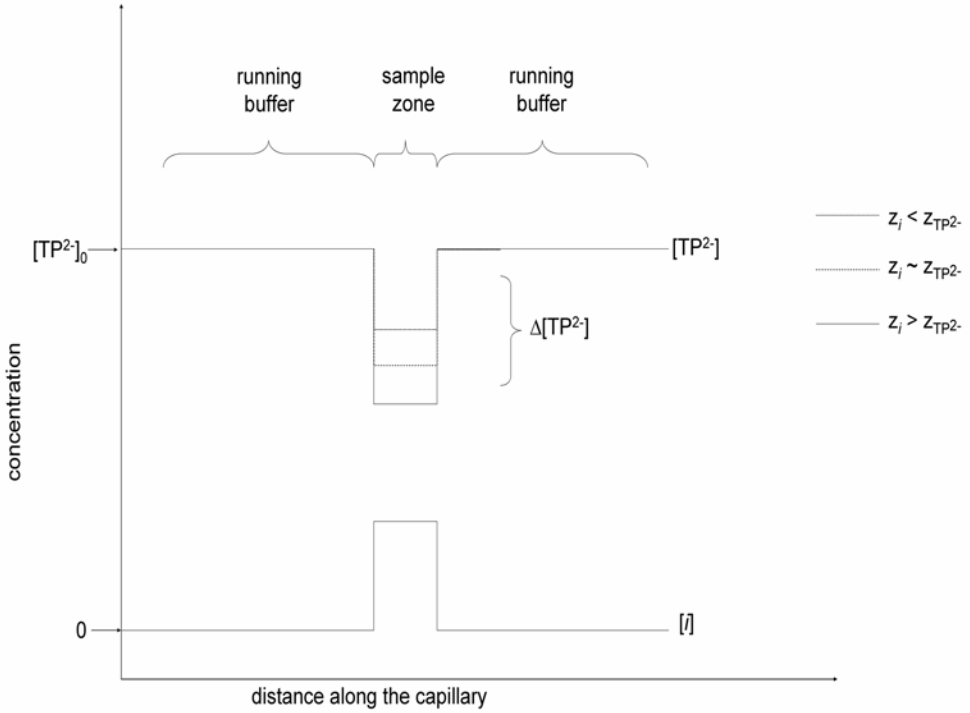

Shapes of Peaks. Triangular peaks observed in the indirect detection of ions are the result of non-uniform electric fields at the boundaries and within samples zones that originate from the difference in mobility between TPA^{2-} and analyte ions. Scheme 2 illustrates how the shapes of peaks correspond to variations in electrical field (while current is constant).

Scheme 2. Shapes of Peaks Observed in Indirect Detection.

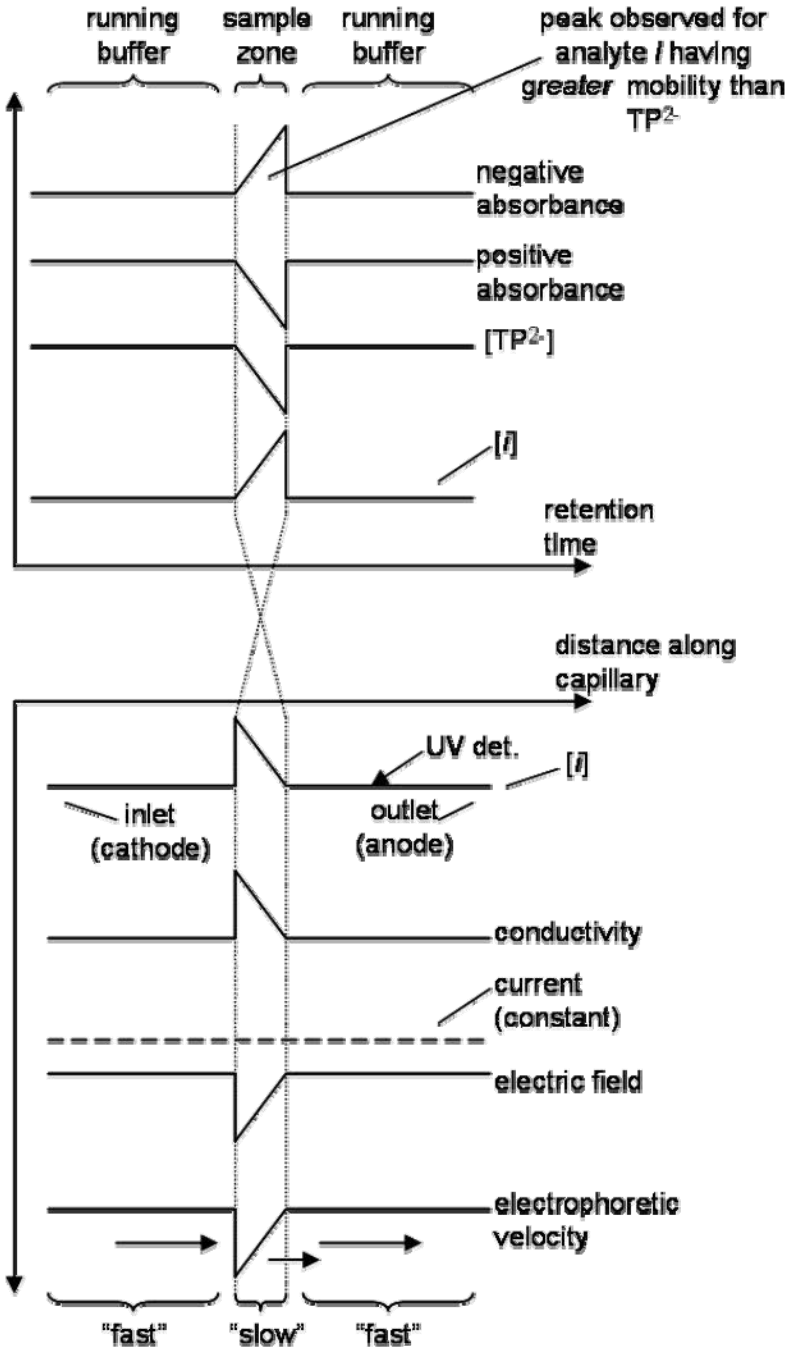

Quantitative Analysis of Peak Areas for $(P_i)_n$ Determined by Indirect UV Absorbance.

Electrokinetic Injection of Anions. We inject anions from sample mixtures into the capillary by dipping the inlet (anode end) of the capillary into the sample and applying a negative voltage to the sample. Equation 2 describes the amount of *i* injected, where $mols_i$ is the number of mols of anion *i* transferred from a sample having a concentration of $[i]_S$; electrokinetic injection is accomplished by applying a voltage ΔV for a duration Δt across a capillary having dimensions *r* (internal radius) and *l* (length). The amount of *i* injected not only depends on the concentration and mobility of *i* (μ_i), but also on the conductivity of the running buffer (κ_0) and the conductivity of the sample (κ_{sample}). The value of κ_{sample} depends on the charge, concentration, and mobility of *all* ions present in the sample.

$$mols_i = [i]_S \cdot \mu_i \cdot \left(\frac{\kappa_0}{\kappa_{sample}} \right) \cdot \Delta t \cdot \Delta V \cdot \left(\frac{\pi r^2}{l} \right) \qquad (2)$$

Derivation of Eq. 2 is based on constraining the current in the sample vial and within the capillary to the same value.

The dependence of $mols_i$ on (κ_0 / κ_{sample}) is a result of discontinuous electrophoresis during electrokinetic injection (in cases where the conductivities of the sample and the running buffer are not the same). When $\kappa_{sample} < \kappa_0$ (e.g., samples dilute in ions), the local electric field (the field in the sample) is stronger than the field in the running buffer; when $\kappa_{sample} > \kappa_0$ (e.g., concentrated samples), the local field is weaker than the field in

the running buffer (illustrated in Scheme 3). The local field forces the migration of anions of the sample into the capillary; the strength of the local field therefore determines the amount of each anion injected and analyzed by CE.

Scheme 3. Non-uniform electrical fields during electrokinetic injections of samples that have conductivity that is greater than (top), equal to (middle), or less than (bottom) that of the running buffer inside the capillary.

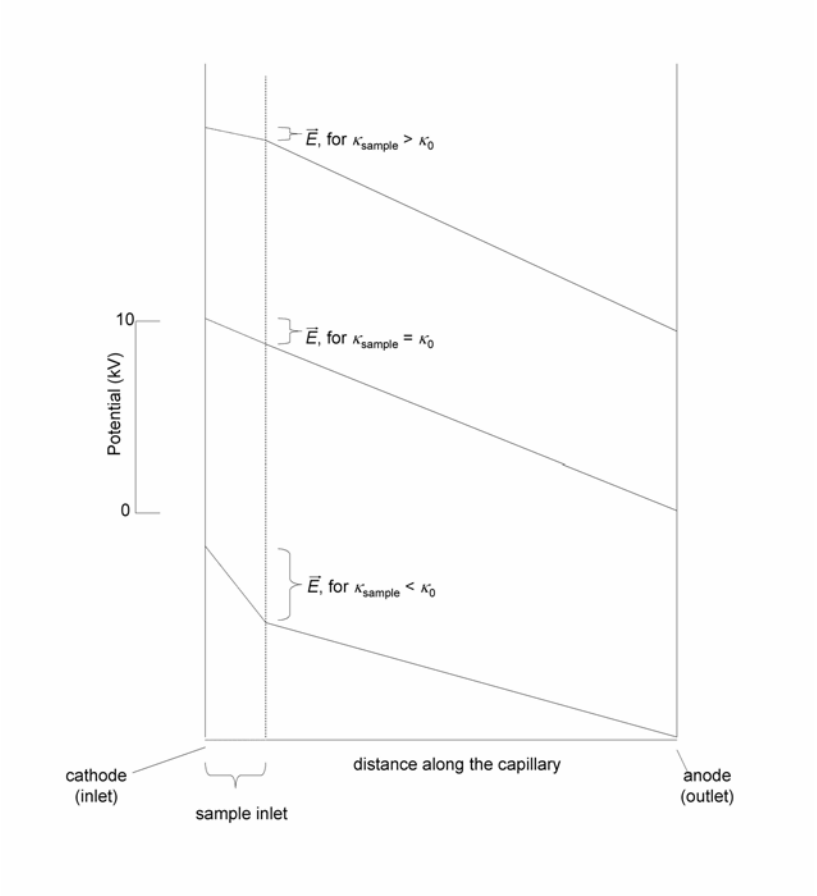

The local field has an important effect on $mols_i$. For example, the amount of P_1 injected from a sample containing 1.0 mM P_1 and 10.0 mM Cl^- will be *less* than the amount of P_1 injected from a sample containing 1.0 mM P_1 and 1.0 mM Cl^- (ΔV, Δt held

constant). The dependence of $mols_i$ on the concentrations and mobilities of *all* ions in the sample (not just *i*) unfortunately prevents us from determining [*i*] by analyzing the size of peak for *i* alone.

Discontinuous electrophoresis can however be useful; the effect of sample stacking, produced by discontinuous electrophoresis, results in the pre-concentration of ions during electrokinetic injection and allows us to analyze dilute samples.

Addition of an internal standard to a sample however enables a way to determine $[i]_S$. The ratio of the amounts of *i* and internal standard ($CH_3SO_3^-$) analyzed by electrokinetic injection and electrophoresis, ($mols_i$ / $mols_{CH3SO3-}$), depends only the concentrations and mobilities of *i* and $CH_3SO_3^-$ (Eq. 3, derived from the expressions for *i* and $CH_3SO_3^-$ and in Eq. 2).

$$\frac{mols_i}{mols_{CH_3SO_3^-}} = \frac{[i]_S}{[CH_3SO_3^-]} \cdot \left(\frac{\mu_i}{\mu_{CH_3SO_3^-}} \right) \qquad (3)$$

Analyzing electropherograms by comparing peak areas for *i* and $CH_3SO_3^-$ allows us to measure the ratio ($mols_i$ / $mols_{CH3SO3-}$), a quantity that is related to $[i]_S$ and known values ($[CH_3SO_3^-]$, μ_i, $\mu_{CH3SO3-}$). Unlike the absolute amounts of *i* and $CH_3SO_3^-$, the ratio ($mols_i$ / $mols_{CH3SO3-}$) is independent of the concentration and mobility of other ions present in the sample. The ratio ($mols_i$ / $mols_{CH3SO3-}$) is also independent of the values and uncertainty in ΔV and Δt.

Analyzing peak areas for $(P_i)_n$ and $CH_3SO_3^-$ to determine $[(P_i)_n]$. The relationship between areas of peaks for $(P_i)_n$ and $CH_3SO_3^-$ and concentrations $[i]_S$ and $[CH_3SO_3^-]_S$ is

predicted by Eq. 7 of the text. Eq. 7 takes into account the contributions from the electrokinetic injection of analyte and internal standard and indirect detection by TP^{2-}, and is derived by combining the expressions for *i* and $CH_3SO_3^-$ in Eq. 1 and Eq. 2.

Figure S1. Identification of Peaks for P_4, P_6, P_7 and P_9 in mixtures of $(P_i)_n$. Traces are for the analysis of mixtures of $(P_i)_n$ (19 mM in total phosphate, pH ~ 8) and added standards for $(P_i)_n$ (2 mM). Mixtures were resolved by CGE at 14.6 kV using capillaries filled with 9.1 % PDMA (w/v) and running buffer (24.0 mM tris, 3.0 mM TP^{2-}, pH = 8.4). Traces are shown in units of mobility relative to the internal standard $CH_3SO_3^-$ (Eq. 6 in the text). Dotted lines for n = 1, 2, 3, 4, 6, 7, and 9 mark peaks for species identified by added standards. The drift in baseline observed in the analysis of samples consisting of $(P_i)_n$ and $(P_i)_7$ was not typical, and result of not re-generating gel-filled capillaries and not using fresh buffer after 5 previous runs (lasting 20 minutes each).

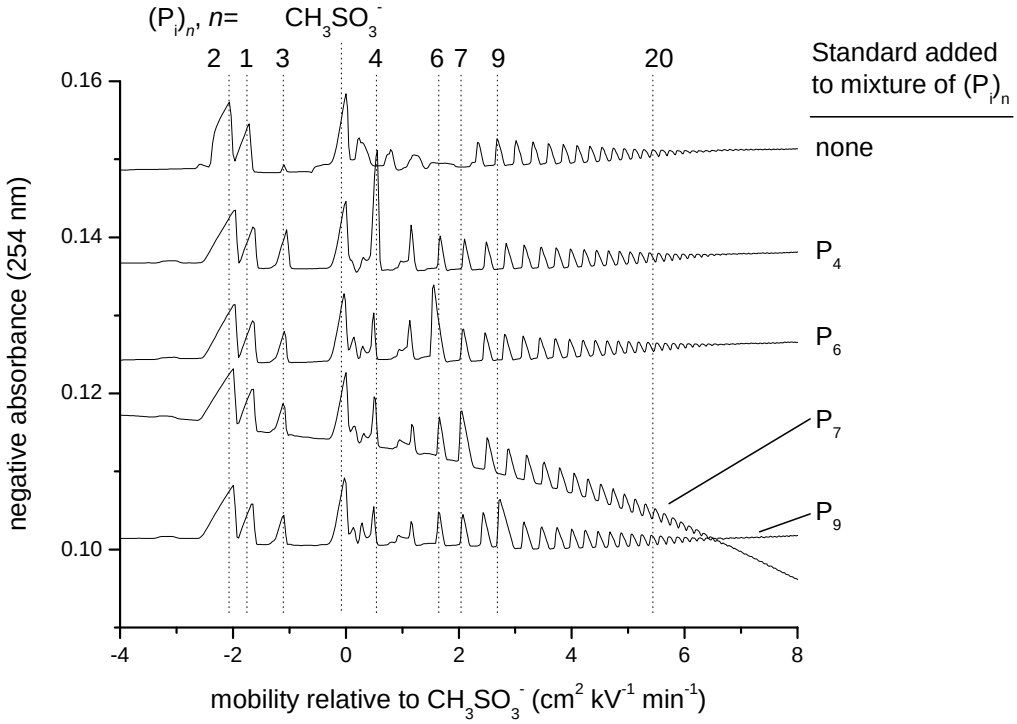

Figure S2. Calibration of Peaks areas to Concentrations of P_1, P_2, and P_3 in CZE.

Data in the plots are for ($A_{(P_i)_n}$ / $A_{CH_3SO_3^-}$), determined in the analysis of samples of P_1, P_2, or P_3, by CZE. Experiments used coated capillaries (57 cm in length, 50 cm between inlet and detector) filled with running buffer (18.0 mM bis-tris, 3.0 mM TP^{2-}, pH = 6.9). Plots show points from all experiments; most samples were prepared and tested once or twice. The slope *m* is for the line determined by fitting the data with adjusted weighting (described in the notes for the text).

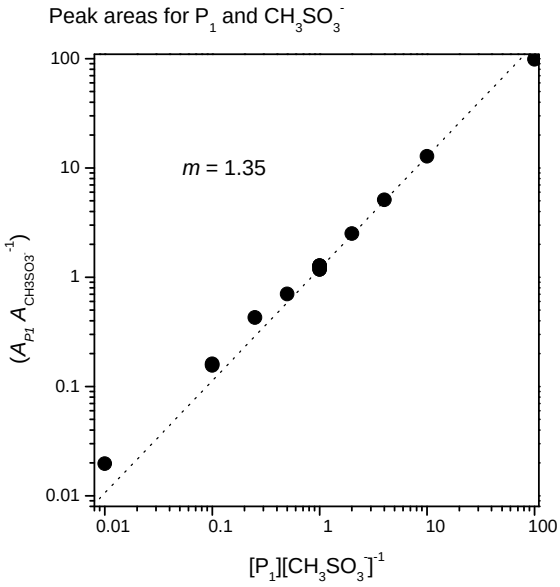

Peak areas for P_2 and $CH_3SO_3^-$

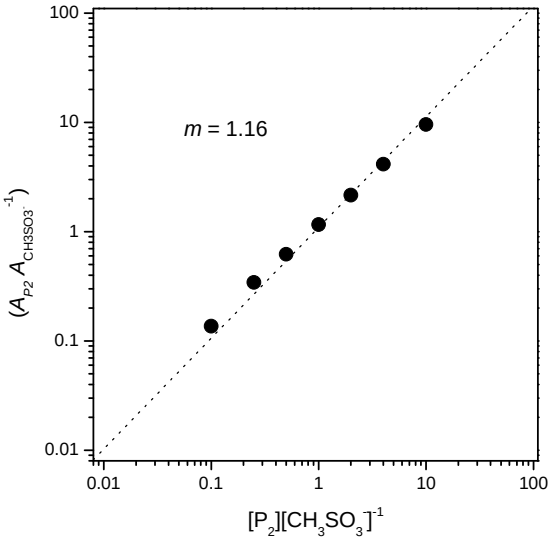

Peak areas for P_3 and $CH_3SO_3^-$

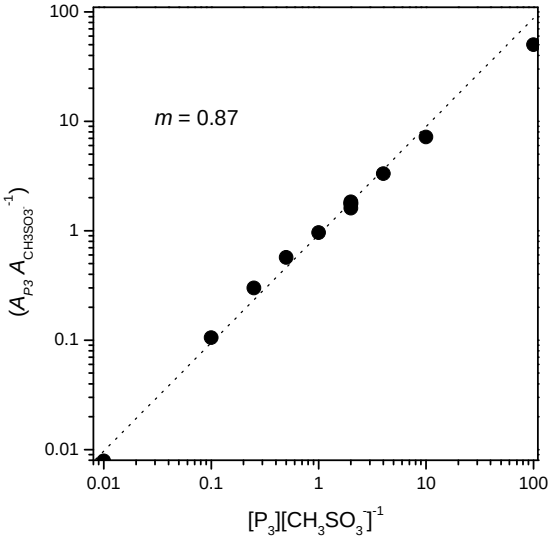

Figure S3. ^{31}P NMR (400 MHz, D_2O) spectra of analytical standards – $(P_i)_4$ - $(P_i)_{10}$ – isolated by ion-exchange chromatography (as NH_4^+ salts).

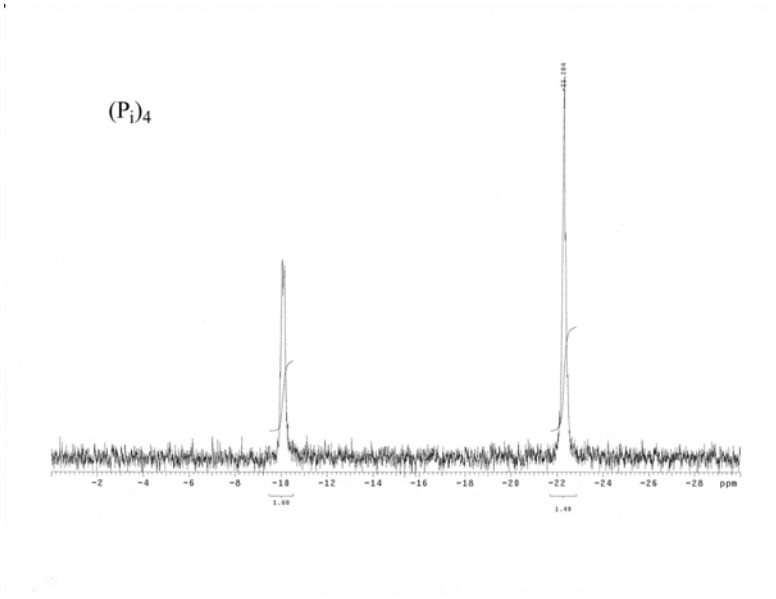

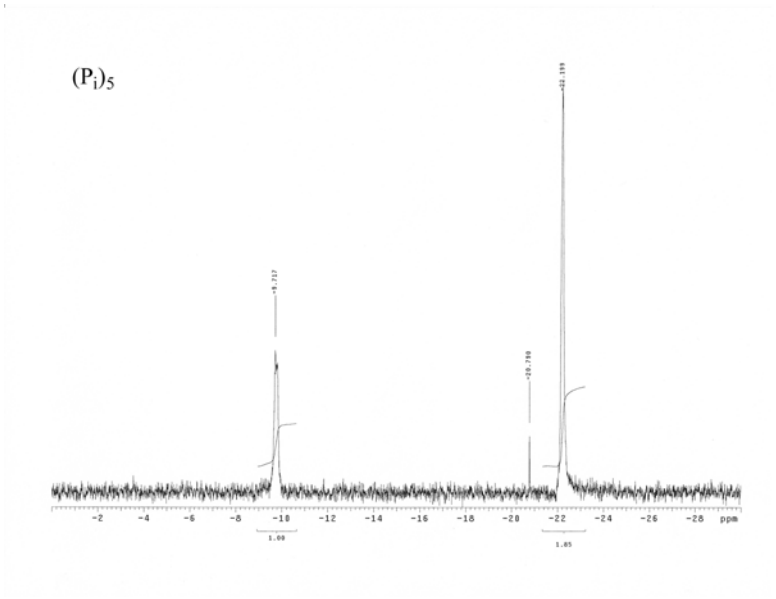

$(P_i)_6$

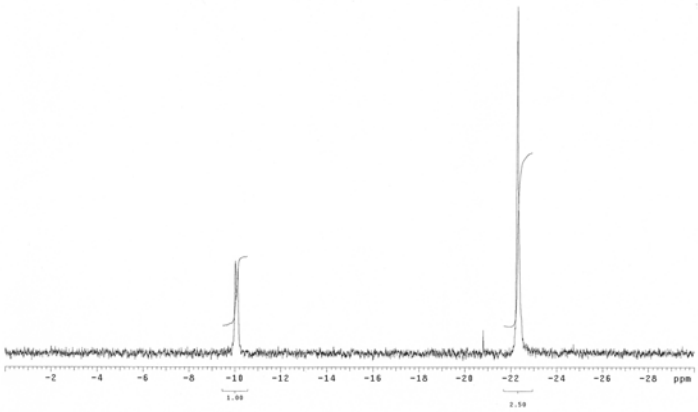
-2
-4
-6
-8
-10
-12
-14
-16
-18
-20
-22
-24
-26
-28
ppm
1.00
2.50

$(P_i)_7$

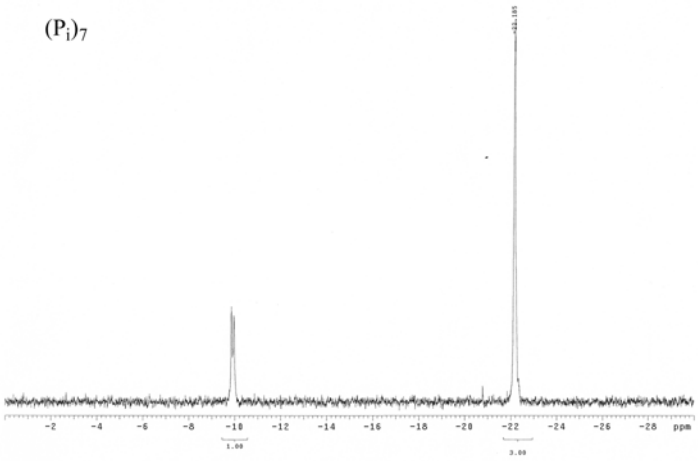
-2
-4
-6
-8
-10
-12
-14
-16
-18
-20
-22
-24
-26
-28
ppm
1.00
3.00

$(P_i)_8$

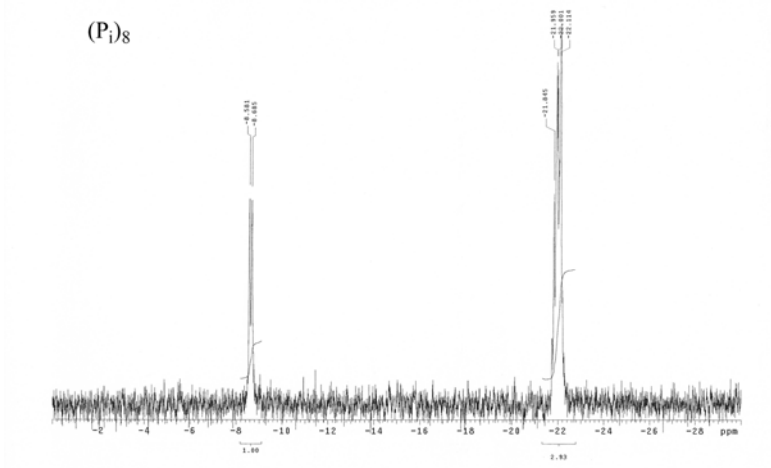
-2
-4
-6
-8
-10
-12
-14
-16
-18
-20
-22
-24
-26
-28
ppm
1.00
2.93

$(P_i)_9$

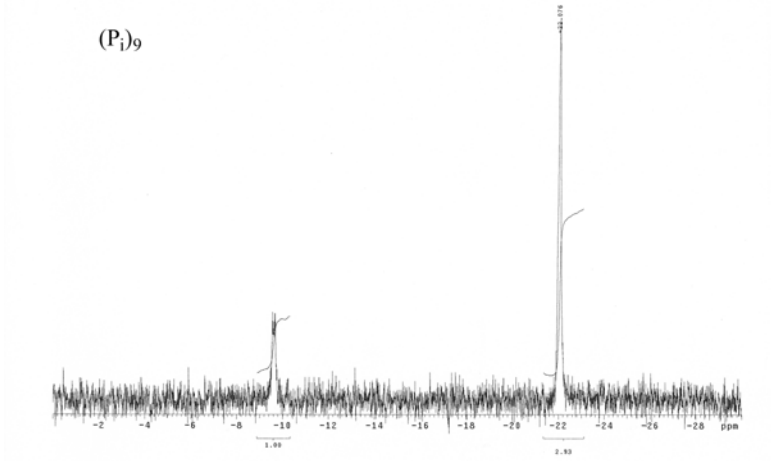
-2
-4
-6
-8
-10
-12
-14
-16
-18
-20
-22
-24
-26
-28
ppm
1.00
2.93

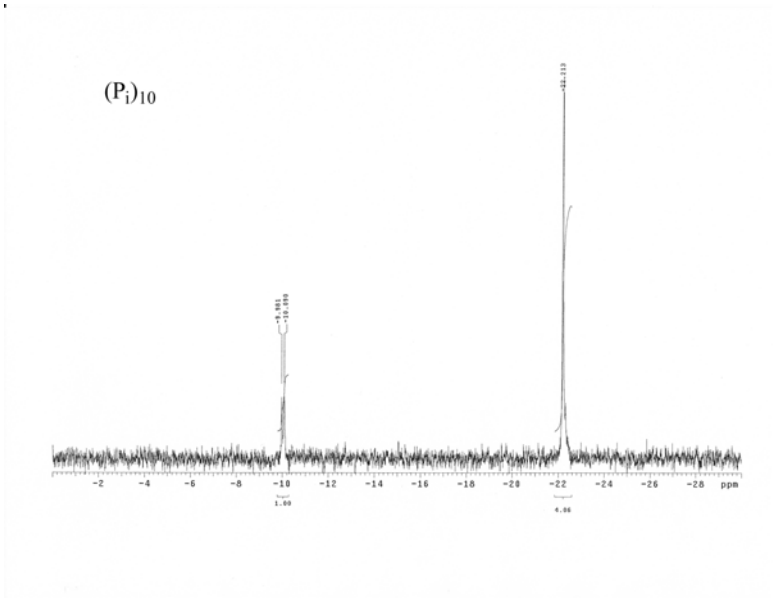

REFERENCES TO THE SUPPORTING INFORMATION.

(1) Rao, N. N.; Gomez-Garcia, M. R.; Kornberg, A. *Annu. Rev. Biochem.* **2009**, *78*, 605-647.
(2) Robinson, N. A.; Wood, H. G. *J. Biol. Chem.* **1986**, *261*, 4481-4485.
(3) Pepin, C. A.; Wood, H. G. *J. Biol. Chem.* **1986**, *261*, 4476-4480.
(4) Ohtomo, R.; Sekiguchi, Y.; Mimura, T.; Saito, M.; Ezawa, T. *Anal. Biochem.* **2004**, *328*, 139-146.
(5) Ogawa, N.; DeRisi, J.; Brown, P. O. *Mol. Biol. Cell* **2000**, *11*, 4309-4321.
(6) Rao, N. N.; Roberts, M. F.; Torriani, A. *J. Bacteriol.* **1985**, *162*, 242-247.
(7) Rashid, M. H.; Kornberg, A. *Proc. Natl. Acad. Sci. USA* **2000**, *97*, 4885-4890.
(8) Gomez-Garcia, M. R.; Kornberg, A. *Proc. Natl. Acad. Sci. USA* **2004**, *101*, 15876-15880.
(9) Phosphoric Acid and Phosphates. *Kirk-Othmer Encyclopedia of Chemical Technology*, 4th ed.; John Wiley & Sons: New York, 1991; Vol.18, pp 669-718.
(10) Poppe, H.; Xu, X. In *High Performance Capillary Electrophoresis: Theory, Techniques, and Applications*; 1 ed.; Khaledi, M., Ed.; Wiley & Sons: New York, 1998; Vol. 146.